Dose conversion coefficients for partial-fan CBCT scans

Helmut Schlattl

Helmholtz Zentrum München – German Research Center for Environmental Health, Institute of Radiation Protection, Ingolstädter Landstr. 1, 85764 Neuherberg

ABSTRACT

Due to the increasing number of cone-beam CT (CBCT) devices on the market, reliable estimates of patient doses for these imaging modality is desired. Cone-beam CT devices differ from conventional CT not only by a larger collimation but also by different recording modes. In this work, it has been investigated whether reliable patient doses can be obtained for CBCT devices in partial-fan mode using pre-computed slices. As an exemplary case, chest CBCT scans for the ICRP reference adult models has been examined. By normalizing organ doses to $\mathrm{CTDI}_{\mathrm{w}}^{100}$, the resulting dose conversion coefficients for CBCT could be well reproduced by precomputed slices, with a relative difference in the effective dose conversion coefficients of less than 10%.

1. INTRODUTION

Driven by faster and larger detector technologies new applications of computed tomography become available. Using flat-panel detectors, cone-beam CT devices (CBCT) entered the market[1] in various fields as in image-guided radiation therapy, angiography or dental radiology. Presently, CBCT devices of x-ray therapy units like Varian OBI or Elekta XVI therapy have a coverage of up to nearly 30 cm.[2] Many CBCT devices can operate in two different modes denoted as partial- and full-fan mode. The two modes are characterized by an asymmetric field with a complete 360°-rotation and a symmetric field with partial rotation, respectively.

For multi-slice CT it has been shown that a suitable normalization quantity for CT dose conversion coefficients (DCC) is $\mathrm{CTDI}_{\mathrm{vol}}$ because then organ DCC are only weakly depending on CT model[3] and tube voltage.[4,5] For CBCT the analogue quantity is $\mathrm{CTDI}_{\mathrm{w}}^{100}$. Since the integration length of 10 cm is not sufficient to cover the whole cone beam and the corresponding scatter radiation, $\mathrm{CTDI}_{\mathrm{w}}^{100}$ is not suitable as a direct CBCT dose descriptor. Nevertheless, it is applicable as a normalization quantity for DCC, since the property of $\mathrm{CTDI}_{\mathrm{w}}^{100}$ to only weakly depend on CT model and tube voltage is not influenced by the integration length.

The geometrical difference to conventional CT devices influences the computation of patient organ doses. In this article, the feasibility to compute patient organ doses using pre-computed slices like in a previous work[5] is examined for the partial-fan mode. For this purpose, it is examined whether also for this case normalizing organ doses to $\mathrm{CTDI}_{\mathrm{w}}^{100}$ is appropriate not only for multi-slice CT,[3,4] but also for CBCT.

2. MATERIALS AND METHODS

The male and female adult ICRP/ICRU reference computational models,[6] denoted as "RCP-AM" and "RCP-AF", respectively, are chosen as reference patients. In a first step, axial slices with tube voltage of 120 kV have been simulated covering the whole body. With the slice thickness of RCP-AM (RCP-AF) being 8 mm (4.84 mm), the axial slices have been chosen to have a collimation of 8 mm (4.84 mm), too, and to be aligned with the model slices. The shape and thickness of the x-ray filtration ("bow-tie filter") corresponds to a Siemens Sensation Cardiac 16 (Siemens Medical Solutions, Forchheim, Germany) with focus to isocenter distance (FID) of 57 and a field of view of 50 cm at the isocenter distance.* From these simulations result organ dose conversion coefficients using air kerma at the axis as reference (K_{a}), denoted as $\mathrm{DCC}_i^{\mathrm{K}}$ (i simply numbers the different slices).

In a second step, chest CBCT examinations have been simulation with the same models. The x-ray tube is positions at a phantom height of 134.5 and 130 cm for RCP-AM and RCP-AF, respectively. The geometrical properties chosen are

E-mail: helmut.schlattl@helmholtz-muenchen.de

*Details of filter material and shape are the proprietary of the manufacturer and cannot be disclosed.

Medical Imaging 2017: Physics of Medical Imaging, edited by Thomas G. Flohr, Joseph Y. Lo, Taly Gilat Schmidt, Proc. of SPIE Vol. 10132, 1013241 · © 2017 SPIE
CCC code: 1605-7422/17/$18 · doi: 10.1117/12.2250571

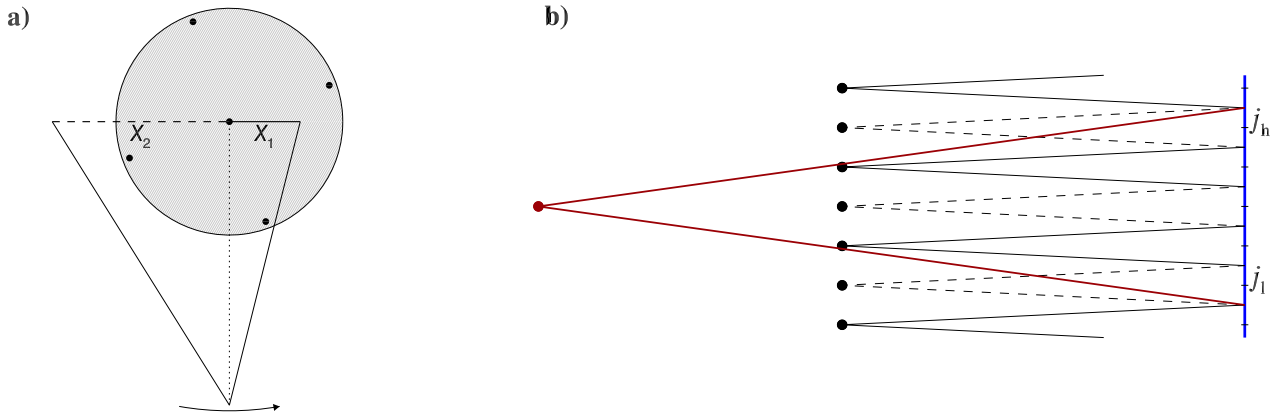

Figure 1. a) Illustration of partial-fan scan mode. b) Illustration of cone-beam combining, where the black solid and dashed lines indicate the cone beam of the axial slices (strongly exaggerated) and the red solid line the cone beam of the CBCT. The blue line represents the isocenter. The dose conversion coefficients of those slices which overlap with the CBCT in the isocenter, i.e, j_l to j_h, are summed up to yield the dose conversion coefficients of the CBCT.

equal to the on-board imager (OBI) of the Varian x-ray therapy unit (Varian Medical Systems, Palo Alto, USA), i.e., an focus-to-isocenter distance of 100 cm and a collimation of 30 cm at the isocenter.[7] Since no information of the filtration is available for the authors, the same filter as for the Siemens Sensation Cardiac 16 has been taken. Note that due to a larger focus-to-isocenter distance, the fan-angle of the Varian OBI is smaller than that of the Siemens Sensation Cardiac 16, and thus the filter thicknesses differ along the fan projection at the isocenter despite the same bow-tie filter being assumed. In addition to the partial-fan mode with collimator blade positions X_1 and X_2 being 2.6 and 23.9 cm (see Fig. 1a), an artificial full-fan simulation has been performed with $X_1 = X_2 = 23.9\,\mathrm{cm}$, as an intermediate step from full-fan multi-slice to partial-fan cone-beam CT. The resulting organ dose conversion coefficients use (again) K_a as reference.

In a third step, $\mathrm{CTDI}_\mathrm{w}^{100}/K_\mathrm{a}$-values are computed using a virtual CTDI body phantom with a diameter of 32 cm and a length of 15 cm. The phantom is represented by voxels with an in-plane resolution of $0.5 \times 0.5\,\mathrm{mm}^2$ and a slice thickness of 2.5 cm and consist of perspex with a density of $1.19\,\mathrm{g\,cm}^{-3}$. Apart from the top- and bottommost slice, the slices contain 4 holes at the edge and 1 hole in the centre of 1 cm in diameter as described in IEC 60601-2-44[8] to account for the position of the 10 cm long pencil ionisation chambers in a real setup (see Fig 1a). In a real setup, a pencil ionisiation chamber is inserted in each hole subsequently, while the remaining holes are filled with a perspex pin. To mimic this procedure in a single simulation, the holes are filled with air of an artificial density of $1.19\,\mathrm{g\,cm}^{-3}$. This way, the absorbed dose is equal to air and the transmission is close to perspex for typical CT tube voltages of 80 kV and higher. Besides, with this density a better statistic uncertainty can be reach with less histories than with actual dry-air density of $1.2 \times 10^{-3}\,\mathrm{g\,cm}^{-3}$.[9] Thus, with 40 million photon histories, coefficients of variance of less than 0.2% could be reached for $\mathrm{CTDI}_\mathrm{w}^{100}/K_\mathrm{a}$.

$\mathrm{CTDI}_\mathrm{w}^{100}$ is given by

$$\mathrm{CTDI}_\mathrm{w}^{100} = \frac{1}{3}\mathrm{CTDI}_\mathrm{c}^{100} + \frac{2}{3}\mathrm{CTDI}_\mathrm{p}^{100}, \tag{1}$$

where $\mathrm{CTDI}_\mathrm{c}^{100}$ and $\mathrm{CTDI}_\mathrm{p}^{100}$ are the mean doses in the central and peripheral holes, respectively, integrated over a length of 100 mm. The collimation was equivalently to the chest CBCT set to 30 cm. The different FID and fan characteristics simulated are summarized in Table 1.

The combination of $\mathrm{DCC}_i^\mathrm{K}$ for the chest CBCT examination is performed analogue to conventional CT[10] in a fourth step. In the referenced work, the slice range indices $i \in (j_l, j_h)$ for the summation of $\mathrm{DCC}^\mathrm{K}{}_i$ are determined by the scan area of a conventional CT. For CBCT the scan area is determined by the area covered by the cone (see also Fig 1b for illustration). Note that generally the fluence per particle on the axis depends on the angle of the impinging particle, which would need to be accounted for when summing up $\mathrm{DCC}_i^\mathrm{K}$. Since the edge of the cone is inclined only by about 8.5°, the fluence of those particles would be just 1.01 ($= 1/\cos(8.5°)$) times higher than of those in the centre of the cone. Thus, this correction is neglected in this work.

FID (cm)	fan characteristic: full fan $\mathrm{CTDI}_{\mathrm{c}}^{100}/K_{\mathrm{a}}$	full fan $\mathrm{CTDI}_{\mathrm{p}}^{100}/K_{\mathrm{a}}$	full fan $\mathrm{CTDI}_{\mathrm{w}}^{100}/K_{\mathrm{a}}$	partial fan $\mathrm{CTDI}_{\mathrm{c}}^{100}/K_{\mathrm{a}}$	partial fan $\mathrm{CTDI}_{\mathrm{p}}^{100}/K_{\mathrm{a}}$	partial fan $\mathrm{CTDI}_{\mathrm{w}}^{100}/K_{\mathrm{a}}$
57	0.0767	0.155	0.129	0.0591	0.0986	0.085
100	0.0838	0.188	0.153	0.0607	0.113	0.095

Table 1. Various $\mathrm{CTDI}/K_{\mathrm{a}}$ in Gy/Gy for a collimation of 30 cm in the different scenarios of this work.

Finally, the various $\mathrm{DCC}^{\mathrm{K}}$ obtained are multiplied by the appropriate $\mathrm{CTDI}_{\mathrm{w}}^{100}/K_{\mathrm{a}}$,

$$\mathrm{DCC}^{\mathrm{CT}} = \mathrm{DCC}^{\mathrm{K}} \frac{K_{\mathrm{a}}}{\mathrm{CTDI}_{\mathrm{w}}^{100}},$$

yielding $\mathrm{DCC}_{\mathrm{sli}}^{\mathrm{CT}}$ for the combined slices at FID of 57 cm, and $\mathrm{DCC}_{\mathrm{ff}}^{\mathrm{CT}}$ and $\mathrm{DCC}_{\mathrm{pf}}^{\mathrm{CT}}$ at $\mathrm{FID} = 100\,\mathrm{cm}$ for (artificial) full-fan and partial-fan CBCT, respectively.

3. RESULTS AND DISCUSSION

3.1 $\mathrm{CTDI}_{\mathrm{w}}^{100}/K_{\mathrm{a}}$

A summary of $\mathrm{CTDI}_{\mathrm{w}}^{100}/K_{\mathrm{a}}$ for the different simulation with the CTDI body phantom is found in Table 1. Since the fan-angle covering the CTDI body phantom is smaller for 100 than for 57 cm, and the bow-tie filtration generally increases with increasing fan-angle, the x-ray filtration at the CTDI body edge is smaller for $\mathrm{FID} = 100\,\mathrm{cm}$. Consequently, the peripheral holes of the CTDI phantom are exposed, on average, to less filtered radiation, leading to a higher $\mathrm{CTDI}_{\mathrm{w}}^{100}/K_{\mathrm{a}}$-value for $\mathrm{FID} = 100\,\mathrm{cm}$ compared to $\mathrm{FID} = 57\,\mathrm{cm}$.

In partial-fan mode not all four peripheral holes are exposed directly to radiation simultaneously, such that $\mathrm{CTDI}_{\mathrm{w}}^{100}/K_{\mathrm{a}}$ is smaller in partial-fan compared to full-fan mode. It is worth noticing that the reduction of $\mathrm{CTDI}_{\mathrm{p}}^{100}/K_{\mathrm{a}}$ from full- to partial-fan mode is consderably less than a factor 2, as one could expect from a complete one-sided field with $X_1 = 0$. Thus, even with X_1 being only about 1/10 of X_2, scatter radiation from the X_1-side significantly contributes to the dose in the peripheral (and central) holes.

3.2 Dose conversion coefficients

In Figs. 2 and 3 the organ $\mathrm{DCC}^{\mathrm{CT}}$ of the combined slices and artificial full-fan CBCT are compared with those of the partial-fan CBCT for RCP-AM and RCP-AF, respectively. The artificial full-fan mode and the combined slices cover the same axis range, such the the observed difference between $\mathrm{DCC}_{\mathrm{ff}}^{\mathrm{CT}}$ and $\mathrm{DCC}_{\mathrm{sli}}^{\mathrm{CT}}$ are caused by the inclined field of the CBCT which is not represented in the combined slices. As not unexpected, the highest differenced between $\mathrm{DCC}_{\mathrm{ff}}^{\mathrm{CT}}$ and $\mathrm{DCC}_{\mathrm{sli}}^{\mathrm{CT}}$ can be observed for organs at the edge of the cone, like thyroid, which are only partly exposed directly. Similarly organs which extend considerably beyond the x-ray field like skin and muscle tissue also show significant differences between $\mathrm{DCC}_{\mathrm{ff}}^{\mathrm{CT}}$ and $\mathrm{DCC}_{\mathrm{sli}}^{\mathrm{CT}}$ as their exposed portion for combined slices is not fully equal to that in cone-beam geometry and the organ distribution with height is not homogenous.

A special case it the male glandular breast tissue which covers only 3 voxel slices, has an (artifical) almost rectangular shape in the sagittal plane, and is close to the body's periphery. For this organ $\mathrm{DCC}_{\mathrm{sli}}^{\mathrm{CT}}$ always underestimates $\mathrm{DCC}_{\mathrm{ff}}^{\mathrm{CT}}$, even for smaller cone-beams. This can be understood when comparing small cones with cranio caudal (=z) coverage equal to 3 and 5 slices (i.e., 24 mm and 32 mm) centred at the height of the male glandular breast tissue. When combining 3 slices $\mathrm{DCC}_{\mathrm{sli}}^{\mathrm{CT}}$ would be close to $\mathrm{DCC}_{\mathrm{ff}}^{\mathrm{CT}}$ as the cone does not extend beyond the breast-tissue slices. When combining 5 slices, only the $\mathrm{DCC}^{\mathrm{CT}}$of 3 slices would contribute to $\mathrm{DCC}_{\mathrm{sli}}^{\mathrm{CT}}$ since the x-rays on the top- and bottomost slice do not reach the breast directly. However, the portion of the 5-slice cone impinging on the breast is higher than 3/5. For the reasoning consider only the antero-posterior direction, where the exposure of the breast is highest. For a 3-slice high cone the actual field size at the breast in the z-direction is smaller about 10% smaller than on the axis, such that a further direct exposure of the breast is obtained when extending the cone to a height of 5 slices. This additional exposure of the breast cannot be reproduced by combining slices. In the examined chest CBCT the field is not centred at the height of the breast, such that all x-rays entering the breast are inclined which leads to a difference between $\mathrm{DCC}_{\mathrm{ff}}^{\mathrm{CT}}$ and $\mathrm{DCC}_{\mathrm{sli}}^{\mathrm{CT}}$ of about 25%.

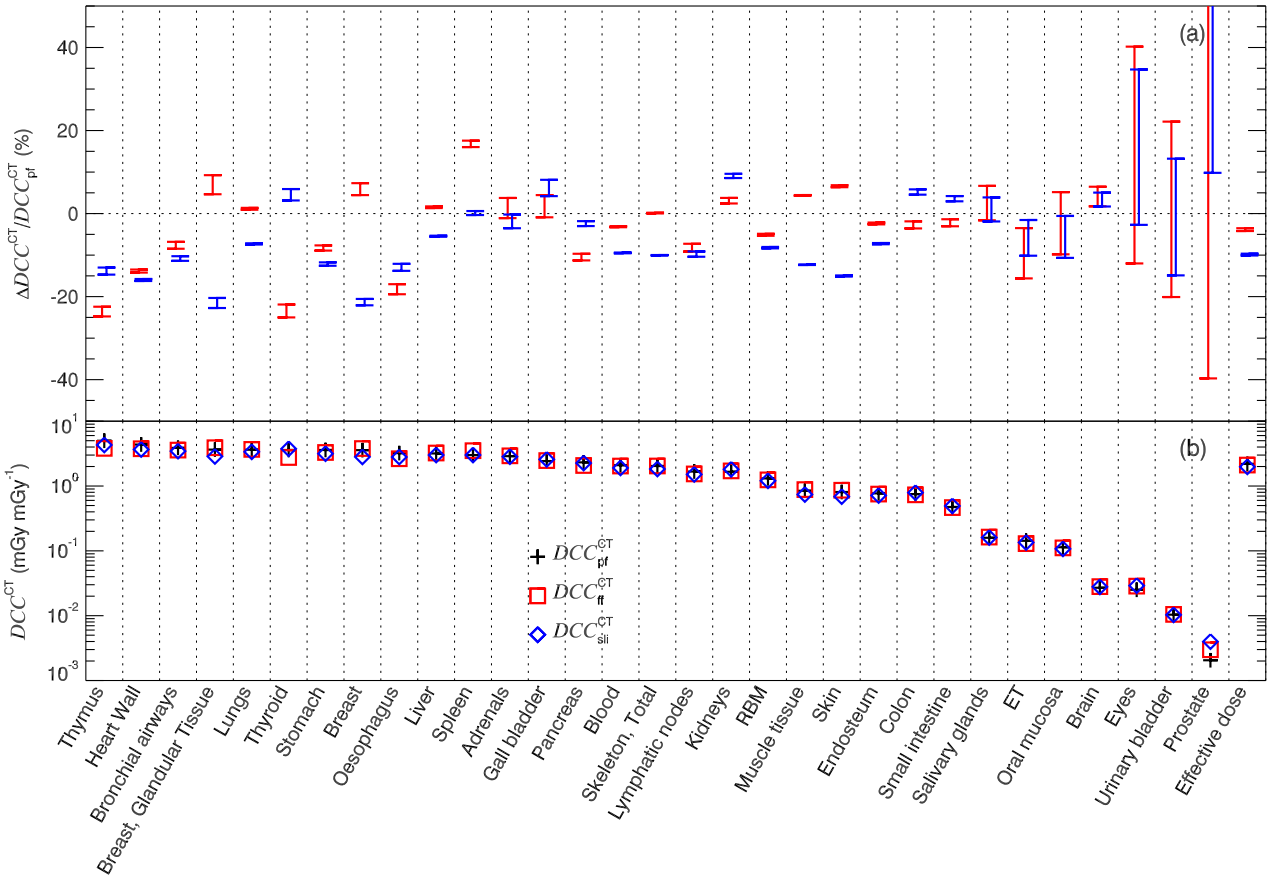

Figure 2. b) Various organ $\mathrm{DCC}^{\mathrm{CT}}$ of RCP-AM for the different scenarios in dose descending order. The effective $\mathrm{DCC}^{\mathrm{CT}}$ is given in the leftmost column. a) Relative difference of $\mathrm{DCC}^{\mathrm{CT}}_{\mathrm{sli}}$ and $\mathrm{DCC}^{\mathrm{CT}}_{\mathrm{ff}}$ compared to $\mathrm{DCC}^{\mathrm{CT}}_{\mathrm{pf}}$ using the same color coding as in b.

It is questionable if the real shape of the male glandular breast tissue in the sagittal plane is reproduced sufficiently accurate with the slice thickness of 8 mm of RCP-AM. It can be expected that the glandular breast tissue in a patient has a less rectangular shape, such that the described additional exposure of the breast in a cone-beam compared to a quasi-parallel beam is less pronounced, and the difference between $\mathrm{DCC}^{\mathrm{CT}}_{\mathrm{ff}}$ and $\mathrm{DCC}^{\mathrm{CT}}_{\mathrm{sli}}$ would actually be smaller.

Also the female glandular breast dose is underestimated when using $\mathrm{DCC}^{\mathrm{CT}}_{\mathrm{sli}}$ instead of $\mathrm{DCC}^{\mathrm{CT}}_{\mathrm{ff}}$. However, the extension of the female breast in z-direction is considerable larger than that of the male breast and its shape in the sagittal plane is rounder, such that the proportion of addition exposure caused by the beam inclination is smaller.

The difference in $\mathrm{DCC}^{\mathrm{CT}}$ between the artificial full-fan and the partial-fan mode is for almost all organs below 20%, for the effective dose about 10% (Figs. 2 and 3). Exceptions are the thyroid and the oesophagus, i.e., organs close to the body axis. Most organs are symmetrically distributed in the body, such that for completely one-sided fan (i.e., $X_1 = 0$) very similar dose conversion coefficients would be expected as for a symmetric fan. Since $X_1 > 0$, organs close to the body axis get more than half of the dose compared to the symmetric case, and thus $\mathrm{DCC}^{\mathrm{CT}}_{\mathrm{pf}}$ is considerably higher than $\mathrm{DCC}^{\mathrm{CT}}_{\mathrm{ff}}$ for thyroid or oesophagus.

Overall Figs. 2 and 3 reveals that in terms of $\mathrm{DCC}^{\mathrm{CT}}$ cone-beam conditions can still be reproduced well with axial slices. The relative differences between $\mathrm{DCC}^{\mathrm{CT}}_{\mathrm{sli}}$ and $\mathrm{DCC}^{\mathrm{CT}}_{\mathrm{pf}}$, or $\mathrm{DCC}^{\mathrm{CT}}_{\mathrm{ff}}$, are for all organs below 25%, thus in the same range as the relative differences between $\mathrm{DCC}^{\mathrm{CT}}_{\mathrm{pf}}$ and $\mathrm{DCC}^{\mathrm{CT}}_{\mathrm{ff}}$.

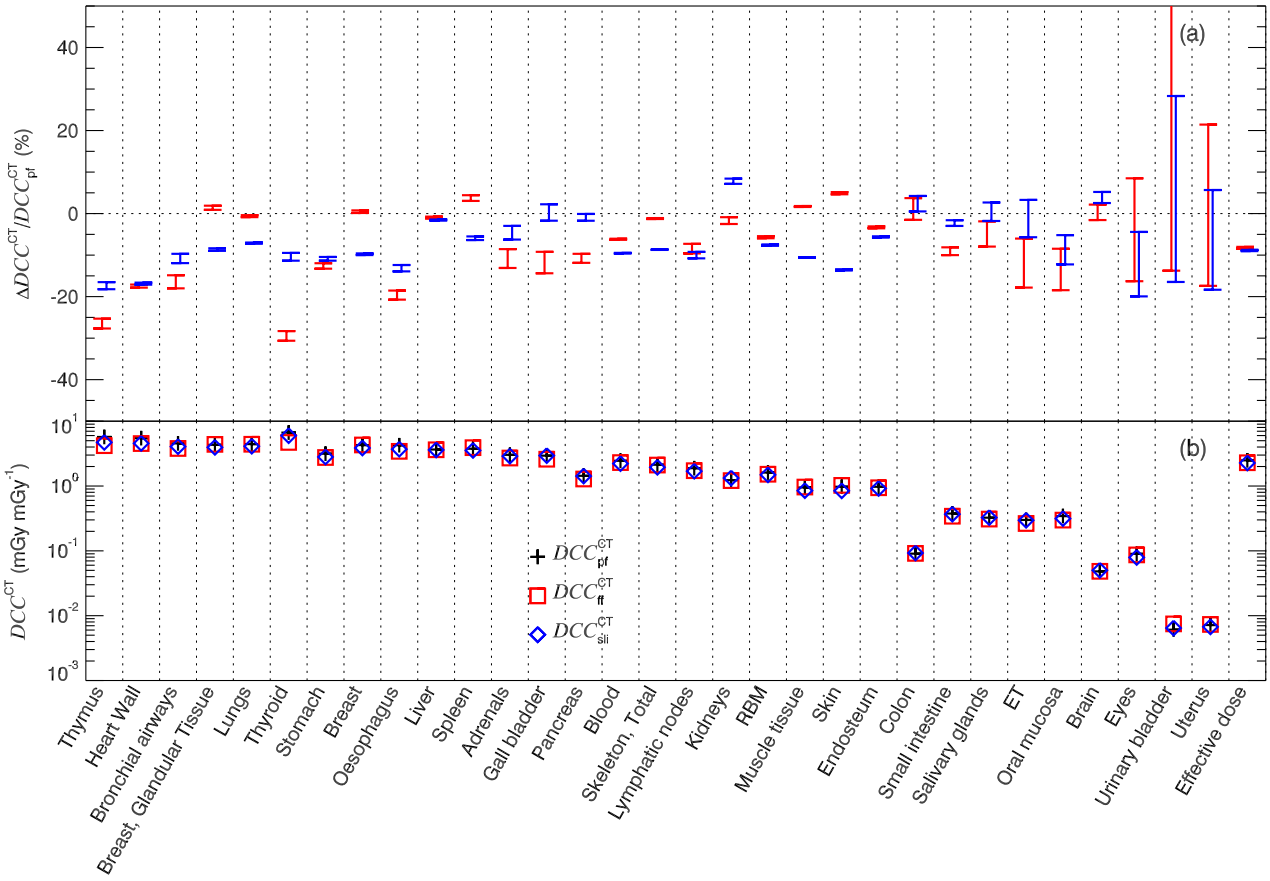

Figure 3. Analogue to Fig. 2 the organ $\mathrm{DCC}^{\mathrm{CT}}$ for RCP-AF.

4. CONCLUSIONS

Organ doses normalized to $\mathrm{CTDI}_{\mathrm{w}}^{100}$ for partial-fan chest CBCT have been computed for the reference male and female phantoms. These values have been compared to $\mathrm{DCC}^{\mathrm{CT}}$ of an artificial full-fan CBCT to demonstrate that organ $\mathrm{DCC}^{\mathrm{CT}}$ only mildly depend on the fan characteristic. It has further been shown that these organ $\mathrm{DCC}^{\mathrm{CT}}$ can be well approximated by combining $\mathrm{DCC}^{\mathrm{CT}}$ of precomputed slices. The highest differences between $\mathrm{DCC}^{\mathrm{CT}}_{\mathrm{pf}}$ and $\mathrm{DCC}^{\mathrm{CT}}_{\mathrm{sli}}$ of at most 25% have been observed for small organs at the edge of the cone (e.g., thyroid), small organs close to the body's periphery whose shape is not well reproduced by the voxel resolution (e.g., male glandular breast tissue, thymus), and organs close to the body axis (e.g., thyroid, oesophagus). For thyroid both effects partly cancel each other, such that only a 10% difference can be observed between $\mathrm{DCC}^{\mathrm{CT}}_{\mathrm{pf}}$ and $\mathrm{DCC}^{\mathrm{CT}}_{\mathrm{sli}}$.

Besides, since the bow-tie filtration for the slices and for the CBCT are different, the good agreement confirms previous findings[3] that organ doses normalized to $\mathrm{CTDI}_{\mathrm{w}}^{100}$ (or $\mathrm{CTDI}_{\mathrm{vol}}$ for multi-slice CT) have only a weak dependence on the bow-tie filtration and thus the scanner type.

REFERENCES

[1] Suzuki, K., Ikeda, S., Ueda, K., Nakamura, T., Okabe, M., Kadomura, T., Baba, R., and Colbeth, R. E., "Development of angiography system with cone-beam reconstruction using large-area flat panel detector," in [*Medical Imaging 2004, Physics of Medical Imaging*], Yaffe, M. J. and Flynn, M. J., eds., **5368**, 488–498, SPIE, Bellingham, WA (2004).

[2] Hioki, K., Araki, F., Ohno, T., Tomiyama, Y., and Nakaguchi, Y., "Monte carlo-calculated patient organ doses from kV-cone beam CT in image-guided radiation therapy," *Biomed. Phys. Eng. Express* **1**(2), 025203 (2015).

[3] Turner, A. C., Zankl, M., DeMarco, J. J., Cagnon, C. H., Zhang, D., Angel, E., Cody, D. D., Stevens, D. M., McCollough, C. H., and McNitt-Gray, M. F., "The feasibility of a scanner-independent technique to estimate organ dose from MDCT scans: Using $CTDI_{vol}$ to account for differences between scanners," *Med. Phys.* **37**(4), 1816–1825 (2010).

[4] Schlattl, H., Zankl, M., and Hoeschen, C., "$CTDI_{vol}$: A suitable normalization for CT dose conversion coefficients at different tube voltages?," in [*Medical Imaging 2012, Physics of Medical Imaging*], Pelc, N., Nishikawa, R. M., and Whiting, B. R., eds., **8313**, 831361, SPIE, Bellingham, WA (2012) .

[5] Schlattl, H., Zankl, M., Becker, J., and Hoeschen, C., "Dose conversion coefficient for paediatric CT examinations with automatic tube current modulation.," *Phys. Med. Biol.* **57**, 6309–6326 (2012).

[6] International Commission on Radiological Protection, "Adult reference computational phantoms," ICRP Publication 110, Elsevier, Amsterdam, The Netherlands (2009).

[7] Abuhaimed, A., Martin, C. J., Sankaralingam, M., Gentle, D., and McJury, M., "An assessment of the efficiency of methods for measurement of the computed tomography dose index (CTDI) for cone beam (CBCT) dosimetry by Monte Carlo simulation," *Phys. Med. Biol.* **59**(21), 6307 (2014).

[8] International Electrotechnical Commission (IEC), [*Medical electrical equipment – Part 2-44: Particular requirements for the basic safety and essential performance of X-ray equipment for computed tomography*], IEC 60601-2-44:2009+AMD1:2012+AMD2:2016, 3.2 ed. (2016). ISBN 978-2-8322-3290-3.

[9] International Commission on Radiological Protection, "Basic anatomical and physiological data for use in radiological protection: reference values," ICRP Publication No 89, Pergamon, Oxford, UK (2002).

[10] Schlattl, H., Zankl, M., Becker, J., and Hoeschen, C., "Dose conversion coefficient for CT examinations of adults with automatic tube current modulation.," *Phys. Med. Biol.* **55**, 6243–6261 (2010).